Cooperative Binding of Magnesium to Transfer Ribonucleic Acid Studied by a Fluorescent Probe†

Dennis C. Lynch‡ and Paul R. Schimmel*

ABSTRACT: The mechanism of cooperative binding of Mg^{2+} to tRNA at pH 7.5 has been studied by means of a naphthyl fluorescent probe covalently attached to the isoleucyl amino moiety of isoleucyl-$tRNA^{Ile}$. The emission of the probe is remarkably sensitive to Mg^{2+} concentration. This sensitivity is due to structural changes in the tRNA induced by binding of Mg^{2+} to "cooperative" sites, as shown by several criteria. Furthermore, it is demonstrated that the probe itself simply monitors but does not cause the structural changes that are observed. The time dependence of the emission changes associated with Mg^{2+} additions to Mg^{2+}-free tRNA has been carefully investigated. The emission changes are biphasic, each phase being associated with a slow unimolecular structural change induced by Mg^{2+} binding to "cooperative" sites. Activation energies for the unimolecular steps are about 30 kcal mol^{-1} and are believed to be associated with the breakdown of "low-salt" structures, this breakdown being induced by Mg^{2+} binding. The cooperativity of Mg^{2+} binding is seen to occur as a "sequential" mechanism in which Mg^{2+} binding steps induce or facilitate subsequent tRNA structure changes. Rate and equilibrium parameters associated with some of the elementary steps in the cooperative process have been obtained.

In solution, tRNA conformation is sensitive to the cation concentration as well as to the temperature (for example, see Yang *et al.*, 1972; Cole *et al.*, 1972). At ambient temperatures, structural transitions which change the shape of the molecule are known to occur rather easily (see for instance, Henley *et al.*, 1966; Tao *et al.*, 1970). These conformational transitions are of interest since they may bear direct relevance to the way in which tRNA fulfills its varied biological role (see Kim *et al.*, 1973). In fact, it is not unreasonable to speculate that conformational changes in tRNA might be a means of modulating the molecule's biological activity.

An inherent difficulty in the characterization of such conformational changes is the translation of gross physical observables (*e.g.*, optical properties), which depend on the aggregate properties of all of the chain elements, into detailed structural information. To avoid such difficulties, a single reporter molecule with unique optical properties may be introduced into a specific site on the tRNA; this avoids the confusion of overlapping spectral contributions, and may reveal information about the specific section of the molecule to which the probe is attached. Of course, when a fluorescent probe is selected, an attempt should be made to minimize the possibility that the probe will interact with the tRNA structure too strongly and thereby perturb the tRNA conformational transitions it is intended to monitor. In such a study, it is also necessary to be sure that the transitions indicated by the reporter molecule are the result of tRNA behavior, and not some trivial effect of the probe itself.

In the experiments described here, a fluorescent reporter molecule, 2-naphthoxyacetic acid (I in Figure 1), was attached to the amino group of isoleucine in isoleucyl-$tRNA^{Ile}$ (*Escherichia coli* B) to give structure IV in Figure 1. Derivatized 3′ mononucleoside and heptanucleotide fragments of $tRNA^{Ile}$ were also prepared (II and III, respectively, in Figure 1). The fluorescence behavior of the naphthoxy group attached to these fragments (II and III) is useful to compare with the behavior of the intact tRNA (IV). The naphthoxy fluorophor is probably one of the simplest fluorescent probes available; it has a relatively small ring system with no substituents. This serves to minimize the possibilities of any strong interactions with the tRNA. In fact, it is shown by a number of control experiments that the probe itself causes no observable perturbation in the tRNA structure.

The fluorescence of the probe was found to be a valuable tool in monitoring structural transitions in $tRNA^{Ile}$. In particular, it was found that the probe gives emission changes in response to the structural changes associated with binding of Mg^{2+} to the *cooperative* or *interacting* divalent ion sites on tRNA (see Cohn *et al.*, 1969; Danchin and Guéron, 1970; Danchin, 1972; Schreier and Schimmel, 1974). This enabled us to perform fluorescence equilibrium and kinetic experiments aimed at elucidating the mechanism and structural effects associated with the cooperative binding of Mg^{2+}. In the following paper (Lynch and Schimmel, 1974), experiments are described in which the probe is used to demonstrate and study a remarkable pH dependence of Mg^{2+} binding arising from "abnormal" ionizations near neutral pH.

Materials and Methods

Preparation and Characterization of Derivatized $tRNA^{Ile}$. *N*-2-Naphthoxyacetylisoleucyl-$tRNA^{Ile}$ was prepared from *E. coli* B unfractionated tRNA (Schwarz BioResearch) by the method of Gillam *et al.* (1968) with only minor modifications in their procedure. The purity of the material was checked by stripping the labeled isoleucine from an aliquot of the tRNA by incubating for 1 hr at pH 9, 1 M Tris, 23°. This incubation removed about two-thirds of the derivative as determined by acid precipitable [^{14}C]isoleucine. The stripped tRNA was then reacylated with [^{14}C]isoleucine of known

† From the Departments of Biology and Chemistry, Massachusetts Institute of Technology, Cambridge, Massachusetts 02139. *Received October 23, 1973.* This work was supported by Grant No. GM 155539 from the National Institutes of Health. This work is taken from the Ph.D. thesis (1973, M.I.T.) of Dennis C. Lynch.

‡ Present address: Division of Biology, California Institute of Technology, Pasadena, Calif. 91109. Predoctoral Fellow of the National Institutes of Health, 1969–1973.

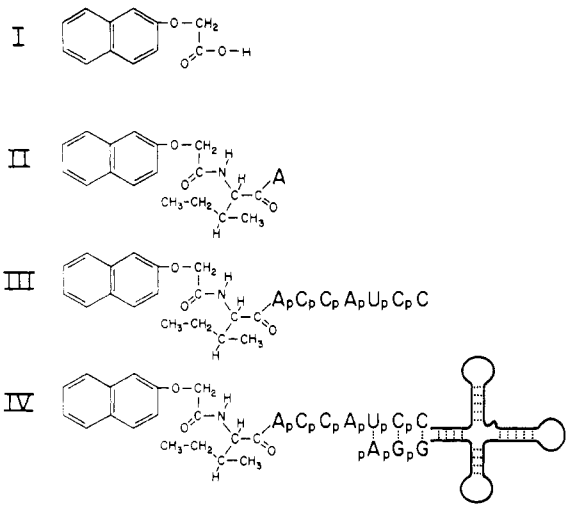

FIGURE 1: Structures of fluorescent derivatives: (I) 2-naphthoxyacetic acid; (II) *N*-2-naphthoxyacetylisoleucyladenosine; (III) *N*-2-naphthoxyacetylisoleucylheptanucleotide; (IV) *N*-2-naphthoxyacetylisoleucyl-tRNA^{Ile}.

specific activity (see Schreier and Schimmel (1972) for aminoacylation conditions). We thus determined that the minimum purity of the pool of IV used in these experiments was *ca.* 70% (based on a theoretical isoleucine incorporation of 1480 pmol/A_{260} unit in 0.1 N NaOH (Yarus and Berg, 1969)). (Since it is difficult to aminoacylate pure tRNA species completely (Bonnet and Ebel, 1972), the purity determined in this manner may be a minimum.) Fluorescence results were independent of the degree of purification, as anticipated.

Aminoacylated tRNAs undergo base-catalyzed hydrolysis to amino acid and tRNA. This hydrolysis proceeds at a significant rate above pH 7. Substitution of the amino group of the amino acid is known to slow this rate substantially. At pH 8.1, a pH higher than any used in actual experiments, *all* of the [^{14}C]isoleucine in [^{14}C]naphthoxyacetylisoleucyl-tRNA^{Ile} remained acid precipitable after 1 hr at 25°. This was taken as evidence of sufficient stability of the aminoacyl linkage of IV to ensure that no deacylation occurred in the normal course of the experiments.

The naphthoxylated isoleucyl-tRNA^{Ile} was shown to be an excellent inhibitor of the aminoacylation reaction of tRNA^{Ile}. This implies that IV binds to the isoleucyl-tRNA synthetase. Binding to the synthetase indicates that IV is in an approximately similar conformation to underivatized tRNA^{Ile} (and isoleucyl-tRNA^{Ile}) under the conditions of the aminoacylation reaction (10 mM Mg^{2+}, pH 8, 37°). Evidence exists that the similar phenoxyacetic acid derivative of isoleucyl-tRNA^{Ile} also binds to isoleucyl-tRNA synthetase at *ca.* pH 5.5, 10°, 10 mM Mg^{2+} (L. Dickson, personal communication). Therefore, it is concluded that IV is probably in a native-like tRNA^{Ile} conformation, in the presence of sufficient Mg^{2+}, over the range of pH 5.5–8.

The unacylated tRNA^{Ile} used in optical density measurements was isolated by A. Schreier of this laboratory and was at least 85% Ile acceptor chains. Other materials employed in the various optical measurements were of the highest quality generally available. The water used in the various buffers was distilled, deionized on a mixed-bed resin, and distilled again in an all glass still (Corning AG-3).

Preparation of I, II, and III. Structure I, 2-naphthoxyacetic acid, was assumed to be formed from its "active" *N*-hydroxysuccinimide ester by spontaneous hydrolysis during preparation of the aqueous solutions. (Spontaneous hydrolysis is minimized prior to the tRNA coupling reaction by adding freshly prepared solutions of the ester in anhydrous tetrahydrofuran directly to the reaction mixture.) Generally, a small amount of the ester was placed in water, or 0.01 M cacodylate buffer at pH 6, and the mixture heated to *ca.* 50° to promote dissolution. The mixture was centrifuged free of undissolved material, and a portion of the supernatant was reheated to ensure that all of the particulate matter was dissolved. These solutions were generally not freshly prepared, but no difference in fluorescence properties was noted over substantial periods of time (weeks).

N-2-Naphthoxyacetylisoleucyladenosine (II) was prepared by treating IV with RNase A. Structure II is the anticipated fluorescent digestion product of RNase A treatment. To verify that larger fluorescent oligonucleotide fragments were not produced, the digestion mixture was chromatographed on a cellulose thin-layer plate (Baker) using a solvent system of 1-butanol, glacial acetic acid, and water (3 : 1 : 1 by volume). In this solvent, all fragments containing one or more phosphates migrate with $R_F < 0.3$ (L. Dickson, personal communication). However, the radioactively labeled fragment containing [^{14}C]isoleucine chromatographed near the solvent front, as expected for II.

The heptanucleotide fragment bearing the pendent naphthoxyacetylisoleucyl moiety (III) was prepared by digesting IV in 0.01 M cacodylate (pH 6.0) for 4 hr at 37° with *ca.* 10 units of T1 ribonuclease per nmole of tRNA. (See Takahashi, 1961 for definition of units.) The digestion mixture was then applied to a BD-cellulose column and eluted in the standard manner (Gillam *et al.*, 1968) using a volatile buffer. All of the radioactivity (in the form of [^{14}C]isoleucine) appeared in the ethanol fraction. This material was subjected to thin-layer chromatography on cellulose plates (E. Merck), using a solvent of 1-propanol, concentrated ammonia, and water (55 : 10 : 35 by volume). This solvent system separates oligonucleotide fragments according to size (U. L. RajBhandary and M. Simsek (1972), personal communication; see also Saneyoshi *et al.*, 1969). (Because of the basicity of the solvent, the naphthoxyacetylisoleucine group is hydrolyzed from the fragment in the process of chromatography.) A single oligonucleotide spot was found, and it chromatographed in the position expected for a heptanucleotide, as adduced from tetra- and hexanucleotide markers which had the ACCA 3′-terminal sequence. This confirmed the expectation that the 3′ fragment from the T1 digestion is a heptanucleotide (Yarus and Barrell, 1971).

Optical Measurements and Characteristics. Measurements of optical density were performed using a Zeiss PMQ II spectrophotometer at a constant slit width of 0.3 mm. The cell block was thermostated for all optical density (and fluorescence) experiments with constant temperatures being maintained to within ±0.2° with a Brinkmann/Lauda K2R circulator equipped with a standard regulator. In experiments where the temperature was varied, a correction was made for thermal expansion. In all titration experiments, corrections were made for dilutions.

Fluorescence measurements were carried out with a Farrand Optical Company Mark I spectrofluorometer equipped with a 200-W mercury–xenon arc lamp (Hanovia). Slits giving a nominal 5-nm bandpass were used in all experiments. Background emission was routinely subtracted and all measurements were corrected for fluctuations in lamp intensity by the use of a standard signal (generally the Raman scattering of the buffer solution). Emission spectra were not corrected for the variation of monochromator or photomultiplier efficiency with wavelength.

Structure I has an emission maximum (uncorrected) of *ca.* 350 nm and an excitation maximum at *ca.* 313 nm (uncorrected) in aqueous solution. Hercules and Rogers (1958) report an excitation maximum of 313 nm and an emission maximum of 350 nm for 2-naphthol, the parent chromophore of I. The naphthoxyl moiety of IV shows a similar emission maximum of 350 nm and an excitation maximum of 313 nm, but excitation at shorter wavelengths is considerably reduced by the high optical density of the tRNA (the A_{260}[1] was about 0.5 for most experiments; this corresponds to a tRNA concentration of about 10^{-6} M). An exciting wavelength of 313 nm was consistently used and all solutions had $A_{313} < 0.02$ so that absorption of exciting light by the solution could be ignored. However, the 313-nm excitation gives rise to Raman scattering of water at 350 nm so that a correction for this scattering had to be made.

In order to protect the tRNA from nuclease degradation and to keep the fluorescence background low, all glassware and cuvets were soaked in chromic acid cleaning solution and extensively rinsed with distilled water. In general, the tRNA solutions prepared for optical measurements were allowed to equilibrate for *at least* 15 min or until reproducible readings could be obtained at 5-min intervals. The latter criterion was used in order to ensure attainment of equilibrium during titrations.

Kinetic Measurements. The change in fluorescence or optical density as a function of time was monitored in kinetic experiments. An aliquot of the starting reactant (generally a cation) was added to the cuvet containing the tRNA. The cuvet was mixed by inversion, and rapidly inserted into the instrument. It was generally possible to obtain a reproducible point at 8 sec in this fashion. The time course was followed by taking individual emission readings at appropriate intervals and checking the standard signal when possible. The data were plotted as logarithm of the signal change *vs.* time. In general, most plots were biphasic (*cf. seq.*). A straight line was drawn through the longer time points and extrapolated back to zero time. This line was subtracted from the total signal at earlier times and the difference was replotted on a semilogarithmic scale. This plot also yielded a straight line. The slopes of these lines yielded the two reciprocal time constants λ_1 and λ_2. The errors in determining the reciprocal time constants for the longer and shorter processes were generally about ± 10 and $\pm 20\%$, respectively.

It was easily possible to obtain time constants for processes with half-times of 6 sec, if the amplitudes were sufficiently large. In one set of experiments, processes having half-times of *ca.* 3 sec were measured. Although the "dead time" of the procedure was *ca.* 8 sec, measurements of somewhat faster rate processes are by no means impossible. Reaction half-times of 0.5 msec were measured with a stopped-flow having a dead time of 2 msec (Pearlmutter and Stuehr, 1968), and in an even more impressive case, Barnett and Jencks (1969) were able to measure half-times as short as 0.7 msec, with a stopped-flow having a dead time of *ca.* 5 msec. Of course, the rates determined for such faster processes will have a larger error (generally $\sim 30\%$) than reported above, and this is reflected in the error bars shown in the figures. These bars show the estimated range in which measured reciprocal time constants might be expected to fall; the observed rates in no case fall outside the range of the bars, and generally they fall within a much smaller range.

[1] Abbreviation used is: A_λ, the absorbance at a wavelength λ of a solution in a 1-cm path-length cell.

In some cases, the measured λ_i's were as close as a factor of 4. In order to ensure that such similar rates could be separated from each other by the graphical procedure utilized, computer simulated data for biphasic process having half-times of 6.4 and 25 sec with relative amplitudes of 1 : 5 (the worst actual case) were generated. Using a selection of time points such as might be obtained in a typical experiment, no difficulty was encountered in correctly determining the two λ_i's *via* the procedure outlined above.

EDTA–Mg^{2+} Buffer System. All of the tRNA solutions used in this work were uniformly treated to remove endogenous Mg^{2+} and other multivalent cations. A concentrated sample of the tRNA ($\sim 10^{-4}$ M) in *ca.* 40 mM EDTA (pH 6) was heated to 60° and allowed to cool to room temperature in about 1 hr. The material was then passed over a Sephadex G-50 fine column, and the tRNA collected in polyethylene snap-cap vials (Eppendorf). (If glass test tubes were used for collection, the tRNA appeared to remove Mg^{2+} adsorbed to the walls of the tubes, and the metal removal procedure was ineffective.) The residual Mg^{2+} remaining after this treatment was less than one Mg^{2+} per tRNA, as verified by atomic absorption. (See Schreier (1973) for a more complete discussion of removal of cations from tRNA.)

In order to perform quantitative Mg^{2+} titrations, it is necessary to know accurately the free Mg^{2+} concentration. At Mg^{2+} concentrations much greater than the tRNA concentration (1 μM), the free and total Mg^{2+} are essentially equal. However, at lower Mg^{2+} concentrations it is necessary to buffer the free Mg^{2+} concentration. This was accomplished with EDTA which was routinely added to all solutions. The apparent dissociation constant for Mg^{2+}–EDTA is 1.6 μM at pH 7.5, 20°.[2] Thus, when the tRNA binds some Mg^{2+}, the free Mg^{2+} concentration is held approximately constant by the EDTA buffering effect. The EDTA also serves to remove other multivalent metal ions that might be contaminants of the buffer systems.

Mg^{2+} binds preferentially to the minus four form of EDTA; since the hydrogen ion pK_H for the final ionization of EDTA is *ca.* $pK_H = 10$,[2] protons are released from EDTA when Mg^{2+} binds at the pH values used in these experiments. In order to maintain a constant pH following Mg^{2+} additions, it was found necessary to make the added Mg^{2+} aliquots somewhat more basic than the solution to which they were added. In addition, the pH buffer was kept 20-fold in excess of the EDTA.

Finally, the use of the EDTA as a Mg^{2+} buffer made it possible to perform kinetic experiments at constant known Mg^{2+} levels. Without such a buffering system it would have been almost impossible to measure rates at low Mg^{2+} concentrations because the free Mg^{2+} concentration would not have remained constant throughout the course of the reaction.

Details of the EDTA and buffer concentrations used in various experiments are given in the figure and table legends.

Results and Treatment of Data

Equilibrium Fluorescence Titrations. The solution conformation of tRNA is known to be sensitive to the presence of

[2] The dissociation constants used for EDTA complexes are taken from Laitinen (1960). They are primarily the work of G. Schwarzenbach and his laboratory. Values of binding constants at temperatures not given by Laitinen (1960) were calculated by using the ΔH value of 7.5 kcal/mol determined in this laboratory for Mg^{2+} binding to EDTA at pH 6.5 (R. Gamble, personal communication). This ΔH value is in excellent agreement with the value of 7.6 kcal mol^{-1} reported by Rialdi *et al.* (1972) for Mg^{2+}–EDTA binding at pH 7.2.

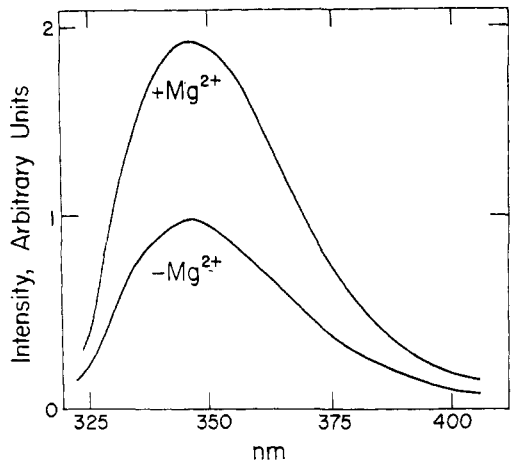

FIGURE 2: Emission intensity (uncorrected; 313-nm excitation) *vs.* wavelength. The lower curve was obtained in 15 mM Na^+, 2 mM Tris, 0.1 mM EDTA, and Cl^- counterion (pH 7.5). Upper curve is the result of adding Mg^{2+} to a final concentration of *ca.* 10^{-4} M in excess of EDTA.

divalent cations (see, for example, Lindahl *et al.*, 1966; Millar and Steiner, 1966; Reeves *et al.*, 1970; Willick and Kay, 1971). The question of interest is whether or not the emission of the fluorescent probe at the 3′-terminus will be sensitive to cations. Figure 2 gives a plot of fluorescence emission *vs.* wavelength both in the presence and absence of Mg^{2+}. It is clear that the addition of Mg^{2+} causes a sizable increase in the fluorescence emission intensity. This change in emission is not due to a trivial interaction of the metal ion with the probe since the addition of Mg^{2+} to fragments II or III produces no emission changes. These results indicate that the probe on the tRNA gives emission changes in response to Mg^{2+}-induced structural changes in the tRNA.

The Mg^{2+}-concentration dependence of the emission changes was investigated by recording the emission at 350 nm at various values of pMg. The results are given in Figure 3a which plots θ (the fractional change in emission) *vs.* pMg, in the presence of 15 mM NaCl at 25°. This plot shows that fluorescence emission has a cooperative dependence on the Mg^{2+} concentration, suggesting that the probe is sensitive to structural changes accompanying the binding of Mg^{2+} to the interacting sites on tRNA (see Cohn *et al.*, 1969; Danchin and Guéron, 1970; Danchin, 1972; Schreier and Schimmel, 1974).

The data in Figure 3a may be further characterized by the empirical Hill equation for the binding of n ligand molecules L to tRNA

$$n\mathrm{L} + \mathrm{tRNA} \rightleftharpoons \mathrm{tRNA}\cdot\mathrm{L}_n \qquad (1)$$

$$K_{app} = \frac{(\mathrm{tRNA})(\mathrm{L})^n}{(\mathrm{tRNA}\cdot\mathrm{L}_n)} = \frac{(1-\theta)}{\theta}(\mathrm{L})^n \qquad (2)$$

and from eq 2

$$\log (1-\theta)/\theta + \mathrm{p}K_{app} = n\,\mathrm{pL} \qquad (3)$$

where $\theta = (\mathrm{tRNA}\cdot\mathrm{L}_n)/[(\mathrm{tRNA}) + (\mathrm{tRNA}\cdot\mathrm{L}_n)]$, and $\mathrm{pL} = -\log[\mathrm{L}]$. A log $(1-\theta)/\theta$ *vs.* pMg plot of the data of Figure 3a is given in Figure 3b. The data conform remarkably well to eq 3 over the range of $0.1 < \theta < 0.9$. From this plot values of $n = 2.3$ and $\mathrm{p}K_{app} = 5.7$ are obtained for the titration in 10 mM Na^+ at 25°.

It was found that the character of the fluorescence Mg^{2+} titrations was sensitive to the concentration of Na^+ and that addition of Na^+ itself was capable of producing emission

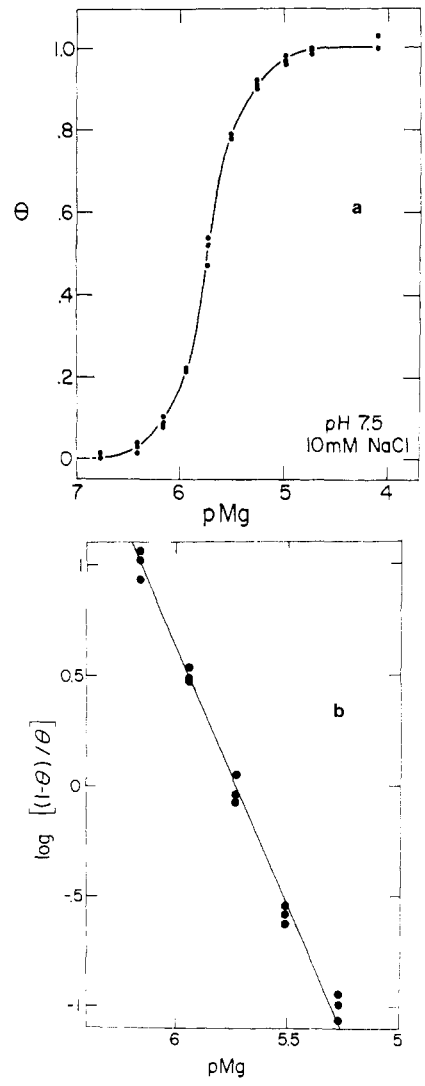

FIGURE 3: (a) Fractional change in emission (θ) *vs.* pMg at pH 7.5, 25° with a buffer of 2 mM Tris, 0.1 mM EDTA, 10 mM Na^+, and Cl^- counterion. Points are from three separate experiments. (b) Plot of log $[(1-\theta)/\theta]$ *vs.* pMg for titration shown in Figure 3a.

changes, although much higher concentrations of Na^+ are required than of Mg^{2+}. Therefore, a series of fluorescence Mg^{2+} titrations was performed at various concentrations of Na^+, and a fluorescence Na^+ titration was performed in the absence of Mg^{2+}. The maximal emissions obtained on addition of Na^+ or Mg^{2+} were the same so that, for example, addition of Mg^{2+} after saturation with respect to Na^+, produced no further fluorescence changes.

The results of several titrations are summarized in Table I. It is clear that Na^+ depresses the empirical index of cooperativity n, but this ion has little influence on $\mathrm{p}K_{app}$. The values of n are consistently equal to or greater than 2.0 at Na^+ concentrations of 25 mM or below. This indicates that under these conditions the fluorescence changes are caused by the cooperative binding of a *minimum* of two or three ions to the interacting sites (see Rossotti and Rossotti, 1961). (Compare with titrations of hemoglobin with oxygen where an n value of 2.7 is obtained even though four interacting sites exist (see Rossi Fanelli *et al.*, 1964).) Thus, the results obtained by fluorescence titration are consistent with several lines of evidence which have indicated that there are four to six interacting sites on tRNA for divalent cations (Cohn *et al.*, 1969; Danchin and Guéron, 1970; Danchin, 1972; Schreier and Schimmel, 1974).

TABLE I: Fluorescence Mg^{2+} Titrations of Labeled $tRNA^{Ile}$ at pH 7.5, 25°.

Na^+ (mM)	pK_{app}	n
<1[a]	~5.9	~2.6
3[a]	5.87 ± 0.1	3.0 ± 0.1
10	5.73 ± 0.04	2.30 ± 0.10
15	5.83 ± 0.08	2.00 ± 0.09
25	5.74 ± 0.05	2.00 ± 0.08
37	5.79 ± 0.06	1.52 ± 0.09
Na^+ titration	1.52 ± 0.05	2.10 ± 0.07

[a] Curve unsymmetric; slope and pK_{app} from initial part which comprised >75% of change. Error limits are 95% confidence limits of least-squares lines. All solutions contained 0.1 mM EDTA, 2 mM Tris, and Cl^- counterion.

The results given in Table I also show that the binding of Na^+ monitored by fluorescence titration is cooperative (n = 2.1) although the binding is about four or so orders of magnitude weaker than that of Mg^{2+}. It is not possible from these results to ascertain whether or not Na^+ and Mg^{2+} are binding to exactly the same loci on the tRNA. However, the fact that entirely comparable emission changes are produced by the two ions argues that they each facilitate a similar structural change in the tRNA, in agreement with the conclusions of Cole *et al.* (1972). The fact that pK_{app} for Mg^{2+} binding is not depressed by Na^+ binding may be due to the cooperativity of the Na^+ binding, *viz.*, Na^+ tends to bind to largely one molecule before binding to another. This leaves many molecules which still have most of their sites available for Mg^{2+} binding, when Na^+ is not saturating.

The uv absorption of tRNA is also affected by cation concentration although the changes are much smaller than those we observe by fluorescence (Fresco *et al.*, 1966; Reeves *et al.*, 1970; Goldstein *et al.*, 1972). The question arises as to the relationship between the fluorescence titration and the analogous uv titration. Figure 4 gives a plot of fractional change θ in uv absorbance (solid line with points) of unacylated $tRNA^{Ile}$ and in emission (dashed line) of derivatized isoleucyl-$tRNA^{Ile}$. The uv changes are very small (~4% at 260 nm (●) and ~7% at 280 nm (○)), but the data are sufficiently accurate to show that the fluorescence and absorption changes are occurring in the same general range of Mg^{2+} concentration. The uv changes are spread over a wider range of Mg^{2+} concentration than are the fluorescence changes, which is probably due to the fact that the absorption is sensitive to structural changes caused by cation association to the strongly binding cooperative sites *as well as* binding to the weaker "independent" sites. The fluorescence changes are clearly associated with the sharply rising and mostly strongly binding phase of the uv titration. This provides further evidence that the probe rather specifically follows just the binding to the interacting class of sites, especially in view of the fact that these sites are known to have the smallest dissociation constants (Cohn *et al.*, 1969; Danchin and Guéron, 1970; Danchin, 1972; Schreier and Schimmel, 1974). Finally, it should be mentioned that a similar uv titration was obtained with derivatized, acylated $tRNA^{Ile}$ (IV) as was obtained with unacylated $tRNA^{Ile}$. This also argues that the fluorescent probe does not significantly perturb the structure and merely monitors structural effects rather than causes them.

Kinetic Studies. In order to determine the sequence of events

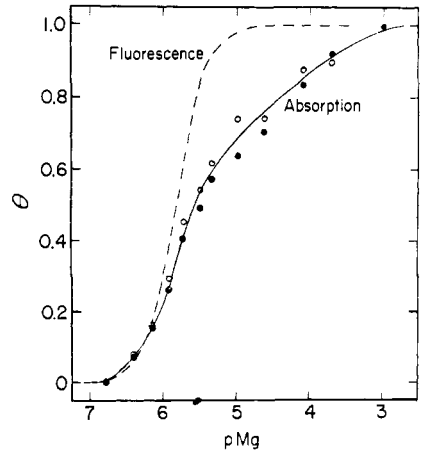

FIGURE 4: Fractional change in absorption (θ) *vs.* pMg at pH 7.5, 25° with a buffer of 2 mM Tris, 0.1 mM EDTA, 15 mM Na^+, and Cl^- counterion: (●) θ for A_{260}; (○) θ for A_{280}. Dashed line is θ for fluorescence changes under same conditions.

associated with the cooperative interaction of Mg^{2+} with tRNA, transient kinetic studies were undertaken. It was found that the addition of Mg^{2+} to an essentially magnesium-free solution of tRNA resulted in transient fluorescence changes which were sufficiently large and slow enough to monitor easily at 20° (in the presence of 15 mM Na^+) without the aid of a stopped-flow device (under these conditions pK_{app} = 5.63 and n = 1.75 in an *equilibrium* titration). Figure 5 gives a plot of emission changes following the addition of Mg^{2+} under these conditions. The inset gives a semilogarithmic plot of the difference between the final emission and the current emission. These data clearly indicate that the kinetic events associated with the emission changes are biphasic. When the longer time portion of the semilogarithmic plot is subtracted from the total signal at earlier time points, the early phase also yields a straight line when the data are replotted. Furthermore, the sum of the emission changes associated with these two phases accounts for the total emission change that occurs. This implies that there are no additional fluorescence kinetic events apart from those associated with these two phases.

A natural question is whether or not there are additional slow kinetic effects associated with binding of Mg^{2+} to tRNA, which are not detected by fluorescence changes. Related to

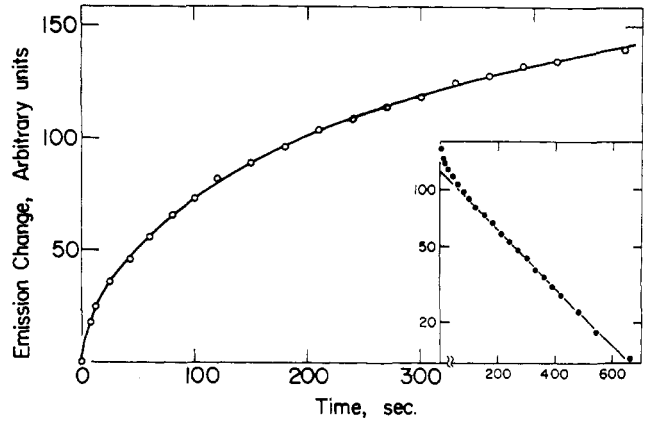

FIGURE 5: Change in fluorescence emission intensity with time following addition of Mg^{2+} at pH 7.5, 20° with a buffer of 2 mM Tris, 0.1 mM EDTA, 15 mM Na^+, and Cl^- counterion. Addition of Mg^{2+} resulted in a final free Mg^{2+} concentration of 2.1 × 10^{-4} M. The inset shows a semilogarithmic plot of the final signal minus the current signal *vs.* time.

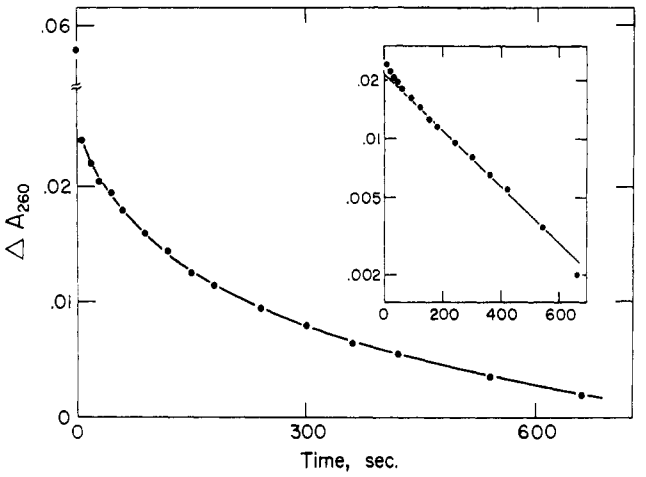

FIGURE 6: Change in A_{260} following Mg^{2+} addition *vs.* time at pH 7.5, 20° with the same buffer as in Figure 5. Inset shows a semilogarithmic plot of change in A_{260} *vs.* time. Mg^{2+} addition was such that free $[Mg^{2+}] = 5 \times 10^{-4}$ M.

this, of course, is the question of whether or not the kinetic effects are somehow uniquely associated with the fluorescent probe and are not actually a reflection of structural changes in the tRNA. (Of course, the latter possibility is somewhat unlikely in view of results cited earlier.) These questions were approached by attempting to examine transient kinetic effects associated with the small uv absorbance changes that occur upon Mg^{2+} addition to unacylated $tRNA^{Ile}$. Although the total change is very small, it was possible to monitor transient changes. The results are shown in Figure 6 which shows that there is a very rapid initial change followed by a much slower phase in the same time range as effects observed by fluorescence. A semilogarithmic plot of the tiny changes associated with the slow phase is linear and has a reciprocal time constant equal to the λ_2 measured by fluorescence under the same conditions. The possibility that a process with a reciprocal time constant equal to λ_1 is also present cannot be ascertained with such small changes. However, experiments at pH 6 do show more clearly that both kinetic effects observed by fluorescence have their counterparts in the uv kinetics of both derivatized *and* underivatized $tRNA^{Ile}$ (Lynch and Schimmel, 1974). We conclude, therefore, that the kinetic effects monitored by the fluorescent probe are associated with the tRNA structure itself and not due to the probe *per se*. Moreover, the uv data indicate that there are no other significant slow kinetic processes beyond those measured by fluorescence effects. The rapid initial change in uv absorbance following Mg^{2+} addition is doubtless due to the initial fast association of Mg^{2+} with tRNA which produces an absorbance change but not a fluorescence change.

Two important control experiments were performed to check further on the nature of the kinetic processes. Since EDTA was employed to buffer the free Mg^{2+} concentration, it is important to verify that it *per se* does not affect the kinetic results. Several experiments were performed in the absence of EDTA (at Mg^{2+} concentrations where EDTA is not needed for buffering) and were found to give the same results as those in the presence of EDTA. Secondly, it was found that the kinetic rates and amplitudes were independent of the order of addition of reactants, *i.e.*, when tRNA instead of Mg^{2+} was used to start the reaction the same results were obtained.

The linearity of the semilogarithmic plots (see above and Figure 5) indicates that the kinetic changes are associated with first-order or pseudo-first-order processes which may be described by the equation

$$\Delta F = A_1 e^{-\lambda_1 t} + A_2 e^{-\lambda_2 t} \tag{4}$$

where $\lambda_1 > \lambda_2$, ΔF is the change in fluorescence emission, and A_1 and A_2 are fluorescence amplitude factors. Information pertaining to mechanism and rate constants is contained in the parameters A_1, A_2, λ_1, and λ_2. These parameters are independent of tRNA concentration over the approximately fivefold variation in tRNA concentration investigated (around 10^{-6} M). This is not surprising since these concentrations are considerably lower than those where concentration dependent phenomena are observed (see Millar and Steiner, 1966). The reaction parameters were also investigated as a function of Mg^{2+} concentration by varying over a wide range the amount of Mg^{2+} which was added to the solution at $t = 0$. These Mg^{2+} additions were almost always sufficient to give saturation of fluorescence (in equilibrium titrations) so that the kinetic effects could be easily followed. At all Mg^{2+} concentrations, biphasic kinetics similar to those shown in Figure 5 were observed, and the λ_i's were found to be concentration dependent.

Figures 7a and b give plots of λ_1 *vs.* $[Mg^{2+}]$ and λ_2 *vs.* $[Mg^{2+}]$, respectively. In both instances, the plots are hyperbolic in character; the λ parameters show a strong dependence on Mg^{2+} at low Mg^{2+} concentrations and eventually reach Mg^{2+}-independent values at higher concentrations. The relative amplitudes of the two processes are such that $A_2 = 4A_1$ at all Mg^{2+} concentrations investigated.

Interpretation of Kinetic Results in Terms of Mechanism. The hyperbolic concentration dependence of reciprocal time constants associated with pseudo-first-order processes suggests that each process is due to a relatively slow unimolecular structural change which is coupled to rapid bimolecular steps, *i.e.*, association of Mg^{2+} with tRNA (Eigen and DeMaeyer, 1963; Hammes and Schimmel, 1970). Several mechanisms of this type were investigated (Lynch, 1973). The simplest one found to be consistent with all of the data is eq 5, where R is

$$\begin{aligned} &R + Mg^{2+} \underset{k_{-1}}{\overset{k_1}{\rightleftharpoons}} X_1 \underset{k_{-2}}{\overset{k_2}{\rightleftharpoons}} X_2 \\ &\qquad\qquad \text{fast} \qquad\quad \text{slow} \\ &X_2 + Mg^{2+} \underset{k_{-3}}{\overset{k_3}{\rightleftharpoons}} X_3 \underset{k_{-4}}{\overset{k_4}{\rightleftharpoons}} X_4 \\ &\qquad\qquad \text{fast} \qquad\quad \text{very slow} \\ &X_4 + Mg^{2+} \rightleftharpoons \cdots \end{aligned} \tag{5}$$

the Mg^{2+}-free form of tRNA (at least as detected by fluorescence) and the X_i's are conformational forms of Mg^{2+}–tRNA complexes. This mechanism envisions that binding of Mg^{2+} to the interacting sites occurs by a rapid initial association of Mg^{2+} to give a complex X_1 which slowly rearranges to a form X_2 which then rapidly adds a second metal ion to yield X_3. This structure very slowly relaxes to another form which can add additional Mg^{2+}. The rate-limiting steps are associated with conformational changes which follow the binding of the first and the second Mg^{2+}, respectively. It is understood, of course, that this mechanism does not rule out the obvious possibility that metal ions other than those depicted may bind to and dissociate from the various structural forms in eq 5, as long as these equilibria are independent of and do not significantly influence those of eq 5.

The reciprocal time constants λ_1 and λ_2 are related to the "slow" and "very slow" unimolecular steps, respectively. The slow step must precede the very slow one in the mechanism

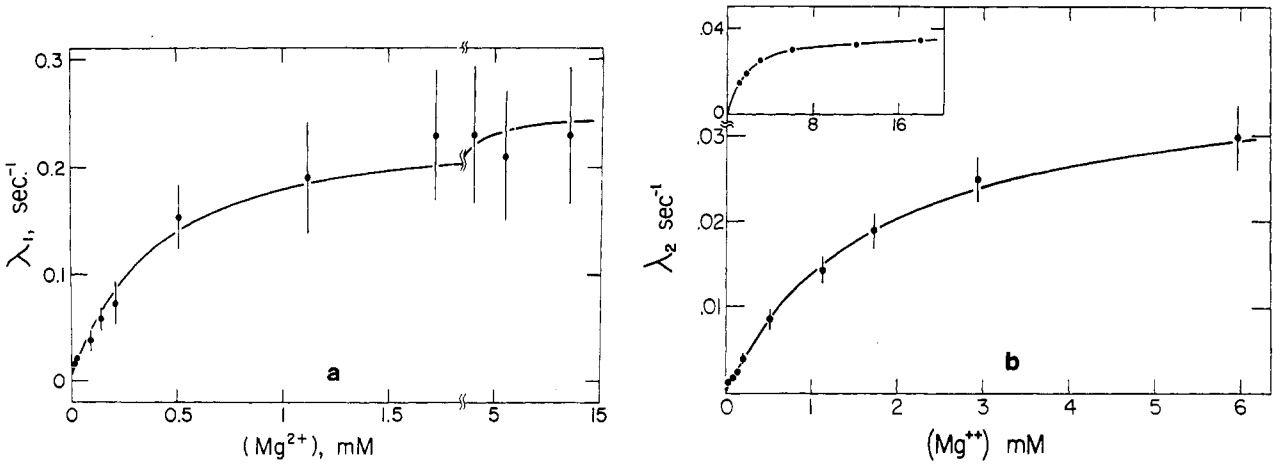

FIGURE 7: (a) λ_1 *vs.* [Mg^{2+}] at pH 7.5, 20°, buffer as in Figure 5. Points are averages of several experiments and the error bars are about ±20% (±30% at plateau; see Materials and Methods). The line is a theoretical curve calculated using eq 8 and values of the parameters listed in Table II. (b) λ_2 *vs.* [Mg^{2+}] at pH 7.5, 20°, buffer as in Figure 5. Points are averages of several experiments, the error bars are about ±10% (see Materials and Methods). The line is a theoretical curve calculated using eq 8 and values of the parameters listed in Table II. The inset shows the same curve carried out to higher [Mg^{2+}] to show the plateau more clearly.

since that is the order in which they occur when Mg^{2+} is added to an essentially Mg^{2+}-free solution of tRNA; moreover, if the very slow step were to precede the slow one, only one kinetic process would be observed.

A simpler mechanism embodying some of the features of eq 5 is one in which one or more Mg^{2+} rapidly binds (at a critical site(s)) and the resulting tRNA species then undergoes a "slow" immediately followed by a "very slow" conformational change, without any intervening Mg^{2+} step between the two structural changes. This type of mechanism will give hyperbolic λ *vs.* [Mg^{2+}] plots for the time constants associated with the two rate-limiting structural changes. However, this kind of scheme fails completely in its ability to quantitatively account for the data of Figures 7a and b (see Lynch, 1973, for further discussion). Equation 5 thus represents the simplest scheme which can account for the data, as is shown below.

The pseudo-first-order rate equations which characterize eq 5 may be derived in a straightforward fashion. The rate equations turn out to be pseudo-first-order because [Mg^{2+}] is held constant by EDTA buffering at low Mg^{2+} concentration, and by virtue of the fact that [Mg^{2+}] ≫ [tRNA] at other concentrations. The equations governing the behavior of the two rate-limiting steps in eq 5 are derived in the Appendix and are given by

$$\begin{aligned} -d\Delta X_1/dt &= a_{11}\Delta X_1 + a_{12}\Delta X_4 \\ -d\Delta X_4/dt &= a_{21}\Delta X_1 + a_{22}\Delta X_4 \end{aligned} \tag{6}$$

where ΔX_i is the deviation at time t of the concentration of X_i from its final equilibrium value and the a_{ij}'s are defined in eq 7a–d. The equilibrium constants K_1 and K_3 are defined

$$a_{11} = \frac{k_2}{1 + K_1/[Mg^{2+}]} + \frac{k_{-2}}{1 + [Mg^{2+}]/K_3} \tag{7a}$$

$$a_{12} = \frac{k_{-2}}{(1 + K_1/[Mg^{2+}])(1 + [Mg^{2+}]/K_3)} \tag{7b}$$

$$a_{21} = \frac{k_4(1 + K_1/[Mg^{2+}])}{(1 + K_3/[Mg^{2+}])} \tag{7c}$$

$$a_{22} = \frac{k_4}{(1 + K_3/[Mg^{2+}])} + k_{-4} \tag{7d}$$

as $K_1 = k_{-1}/k_1$ and $K_3 = k_{-3}/k_3$. The solutions to eq 6 are of the form $\Delta X_i = C_1e^{-\lambda_1 t} + C_2e^{-\lambda_2 t}$ where C_1 and C_2 are constants and λ_1 and λ_2 are given by (see Amdur and Hammes, 1966)

$$\lambda_{1,2} = \frac{(a_{11} + a_{22}) \pm \sqrt{(a_{11} + a_{22})^2 + 4(a_{12}a_{21} - a_{11}a_{22})}}{2} \tag{8}$$

where λ_1 is associated with the positive root and λ_2 with the negative root.

The rate constants k_2, k_{-2}, k_4, and k_{-4} may be extracted from the data of Figures 7a and b by using certain relationships involving λ_1 and λ_2 (Hammes and Haslam, 1968, 1969; Hammes and Schimmel, 1970). These relationships are

$$\lambda_1 + \lambda_2 = a_{11} + a_{22} \tag{9a}$$

$$\lambda_1\lambda_2 = a_{11}a_{22} - a_{12}a_{21} \tag{9b}$$

Limiting forms of eq 9a and b provide four relationships for the four rate constants. Their limiting forms are obtained by substituting the a_{ij}'s from eq 7a–d into eq 9a and b and calculating the high and the low Mg^{2+} limits of these expressions. The results obtained are

$$(\lambda_1 + \lambda_2)_{Mg^{2+}\to\infty} = k_2 + k_4 + k_{-4} \tag{10a}$$

$$(\lambda_1\lambda_2)_{Mg^{2+}\to\infty} = k_2(k_4 + k_{-4}) \tag{10b}$$

$$(\lambda_1 + \lambda_2)_{Mg^{2+}\to 0} = k_{-2} + k_{-4} \tag{10c}$$

$$(\lambda_1\lambda_2)_{Mg^{2+}\to 0} = k_{-2}k_{-4} \tag{10d}$$

Limiting values of the λ_i's are obtained from Figures 7a and b, and these values are then substituted into eq 10a–d to give solutions for the four rate parameters. The remaining parameters K_1 and K_3 are essentially determined by the midpoints of the λ_1 and λ_2 *vs.* [Mg^{2+}] curves, respectively. This is clearly seen when calculated curves of λ_i *vs.* [Mg^{2+}] are generated using eq 8 with the rate constants determined by eq 10a–d. Moreover, if approximate solutions to λ_1 and λ_2 are obtained by assuming that λ_1 and λ_2 are always separated by a factor of 10 or more (which is not always true), these approximate solutions also show that the midpoints of the λ_i *vs.* [Mg^{2+}] curves largely determine K_1 and K_3 (Lynch, 1973).

Values of the six parameters associated with the mechanism of eq 5 are tabulated in Table II. The errors in these parameters are estimated as *ca.* ±20%. The curves of λ_1 and λ_2 *vs.* [Mg^{2+}] calculated with these parameters are given in Figures 7a and b, respectively. Agreement between calculated curves

TABLE II: Kinetic Parameters at pH 7.5, 15 mM Na^+, 20°.[a]

$k_2 = 0.25\ sec^{-1}$	$k_4 = 0.038\ sec^{-1}$
$k_{-2} = 0.0025\ sec^{-1}$	$k_{-4} = 0.000034\ sec^{-1}$
$K_1 = 4.2 \times 10^{-4}$ M	$K_3 = 1.7 \times 10^{-3}$ M

[a] All kinetic experiments at pH 7.5 were done with solutions containing 0.1 mM EDTA, 2 mM Tris, 15 mM Na^+, and Cl^- counterion.

and experimental points is very satisfactory. Since there is some ambiguity in the limiting values of the λ_i's (especially at $[Mg^{2+}] \rightarrow 0$), some adjustment of the parameters is possible. The parameters given in the table are those which give the best agreement between calculated and observed kinetic curves and the calculated and observed equilibrium titration curves (*cf. seq.*).[3]

The results in Table II show that the initial bimolecular association between tRNA and Mg^{2+} is rather weak (*cf.* K_1 and K_3). However, the conformational changes following the initial associations lie far to the right so that the *apparent* or *overall* associations are quite strong. These apparent magnesium association constants are $K_1^{app} = [R][Mg^{2+}]/(X_1 + X_2) = 4.2 \times 10^{-6}$ M and $K_2^{app} = (X_1 + X_2)[Mg^{2+}]/(X_3 + X_4) = 1.5 \times 10^{-6}$ M. Thus the overall association of the second Mg^{2+} is stronger than the first, in keeping with a cooperative mechanism.

Temperature Dependence of Equilibrium and Kinetic Parameters. Further insight into the nature of the structural changes associated with cooperative metal binding, and especially the slow $X_1 \rightleftarrows X_2$ and $X_3 \rightleftarrows X_4$ steps, may be gained by an investigation of the temperature dependence of the rate and equilibrium parameters associated with the various processes. This is not easily accomplished over a wide temperature range, however, because of the extreme temperature dependence of the rates. The data discussed in the previous section were obtained at 20° since the entire λ_i *vs.* $[Mg^{2+}]$ curves could conveniently be obtained at this temperature. The rates become prohibitively slow at temperatures significantly below 20° (*e.g.*, 10 and 15°), making it especially difficult to perform *equilibrium* Mg^{2+} titrations. However, the $[Mg^{2+}] \rightarrow \infty$ plateau of both λ *vs.* $[Mg^{2+}]$ curves was obtained at 10 and 15° thus making it possible to calculate k_2 and k_4 at both temperatures (see below). At temperatures significantly above 20°, the rates become too fast to measure by techniques used here. Moreover, equilibrium titrations are hindered by the enhanced danger of hydrolysis of the aminoacyl linkage at higher temperatures. However, we did obtain the entire λ_2 *vs.* $[Mg^{2+}]$ curve at 25° but the $[Mg^{2+}] \rightarrow \infty$ plateau of the λ_1 *vs.* $[Mg^{2+}]$ curve was too fast to determine at this temperature.

[3] The kinetic data are completely characterized by rate equations (eq 6) which take no account of binding of Mg^{2+} to X_4 in such a way that the $X_3 \rightleftarrows X_4$ equilibrium would be pulled even further to the right. This is a consequence of the small size of k_{-4}. The effect of adding the step

$$X_4 + Mg^{2+} \overset{K_5}{\rightleftarrows} X_5$$

for example, is to modify only the k_{-4} terms in the expressions for the a_{ij}'s such that k_{-4} is replaced by $k_{-4}/(1 + (Mg^{2+})/K_5)$. However, this modification has no significant effect on the calculated curves of Figures 7a and b because the k_{-4} term is negligible compared to the other kinetic parameters. The value of k_{-4} calculated from eq 10c and d is the same whether the additional step(s) is added to the mechanism or not since the value of $(\lambda_1\lambda_2)_{Mg^{2+}\rightarrow 0}$ is unchanged.

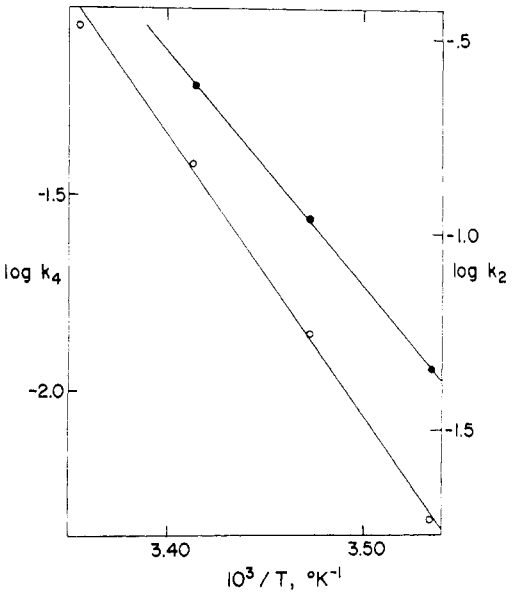

FIGURE 8: Log k *vs.* $1/T$ for k_2 and k_4. Numerical values are listed in Table III. All experiments were at pH 7.5, 15 mM Na^+, 2 mM Tris, Cl^- counterion, and 0.1 mM EDTA.

The high Mg^{2+} plateaus of the λ_i *vs.* $[Mg^{2+}]$ plots can be directly related to k_2 (λ_1 plateau) and k_4 (λ_2 plateau). This is a direct consequence of the fact that $k_4 \gg k_{-4}$. Equations 10a and b can be solved approximately to give

$$\lambda_1 = k_2,\ [Mg^{2+}] \longrightarrow \infty$$
$$\lambda_2 = k_4,\ [Mg^{2+}] \longrightarrow \infty \qquad (11)$$

Figure 8 gives the plots of log k_2 and log k_4 *vs.* T^{-1}, the parameters being obtained as described above (eq 11) at 10, 15, 20, and 25° (k_4 only). Although the temperature interval is small, the marked temperature dependence of the rates gives a good spread in the points. Activation energies for k_2 and k_4 are 27 ± 2 and 33 ± 3 kcal mol^{-1}, respectively. The error limits correspond to the 95% confidence limits of the least-squares lines.

Table III contains a complete summary of the temperature dependence of the various parameters which could be investigated in the presence of 15 mM Na^+. Values of the equilibrium parameters pK_{app}, n, and K_3 are given in addition to the rate constants k_2 and k_4. The value of K_3 at 25° was estimated from the λ_2 *vs.* $[Mg^{2+}]$ plots as described in the Section on Interpretation of Kinetic Results in Terms of Mechanism. Other parameters were not determined for reasons cited above.

The relatively large activation energies associated with the two rate processes suggests that the Mg^{2+}-induced structural changes are quite significant. They might involve the breaking and eventual remaking of several base pairs. For example, Pörschke and Eigen (1971) report that the dissociation of $A_8 \cdot U_8$ helices has an activation energy of 30 kcal mol^{-1} at neutral pH, 0.1 M Na^+. However, the activation energy is quite salt dependent since Craig *et al.* (1971) report a value of 37 kcal mol^{-1} for the dissociation of $A_4 \cdot U_4$ at higher Na^+ concentration (0.25 M). It is not possible to compare directly our activation energies obtained in the presence of Mg^{2+} with those measured in Na^+, but one expects that the activation energies associated with k_2 and k_4 could easily reflect the breaking of several base pairs. On the other hand, the magnitudes of k_2 and k_4 are much smaller than those observed for the dissociation of simple helices (Pörschke and Eigen (1971);

TABLE III: Temperature Dependence of Equilibrium and Kinetic Parameters.[a]

	Temp, °C					
	10	15	20	25	30	E_a (kcal/mol)
k_2 (sec^{-1})	0.045	0.11	0.25			27 ± 2
k_4 (sec^{-1})	0.0046	0.014	0.038	0.085		33 ± 3
K_3 (M)			1.7×10^{-3}	1.4×10^{-3}		
pK_{app}			5.63 ± 0.04	5.83 ± 0.08	5.62 ± 0.06	
n			1.75 ± 0.05	2.00 ± 0.09	1.98 ± 0.07[b]	

[a] All data were obtained in a buffer at 15 mM Na^+, 2 mM Tris, 0.1 mM EDTA, and Cl^- counterion. [b] Curve was unsymmetric.

Craig *et al.* (1971)) so that more complex phenomena are certainly present in the case of tRNA.

The strong temperature dependence of the rate parameters k_2 and k_4 is not reflected in any significant temperature dependence of pK_{app}. This suggests that one or more of the several reverse rate parameters has a sizable activation energy. The small temperature dependence of pK_{app} is in accord with the microcalorimetric results of Rialdi *et al.* (1972) who report $\Delta H = 0 \pm 2$ kcal mol^{-1} for Mg^{2+} binding to yeast $tRNA^{Phe}$. Although the thermodynamic results might lead one to conclude that significant structural changes are not promoted by Mg^{2+} assocation (Rialdi *et al.*, 1972), the large activation energies associated with the kinetic parameters suggest otherwise.

Use of Kinetic Parameters to Calculate Equilibrium Titration Curves. A question of considerable interest is whether or not the kinetic rate and amplitude parameters can be used to reconstruct the equilibrium fluorescence titration curve (*cf.* Figure 3a). To accomplish this, relative fluorescence emissions f_{X_i} must be assigned to each of the species in the mechanism of eq 5. This may be done as follows. The emissions of R and X_1 must be the same since there is no rapid change in emission associated with the initial bimolecular step. The emission change associated with λ_1 therefore represents the overall conversion of $R + X_1$ to $X_2 + X_3$, where X_2 and X_3 must have greater emissions than $R + X_1$. Since the relative amplitude of this first phase is Mg^{2+}-independent over the range of Mg^{2+} investigated (see above), we conclude that the emissions of X_2 and X_3 are equal. This follows from the fact that the ratio of X_2 to X_3 at the completion of the first phase is not constant over the range of Mg^{2+} investigated (see value of K_3 in Table II). The structural change $X_3 \rightarrow X_4$ is thus assumed to bring about the fluorescence change associated with λ_2. Emissions of species formed subsequent to X_4 must then be assumed to be equal to that of X_4. According to these assignments, the fact that the amplitude of the second phase is four times that of the first phase, and the fact that the total Mg^{2+}-induced fluorescence change is 1.8-fold under the conditions of the kinetic experiments (15 mM Na^+, 20°), we obtain

$$f_R = f_{X_1}$$
$$f_{X_2} = f_{X_3} = 1.16 f_R \quad (12)$$
$$f_{X_4} = 1.8 f_R$$

In an equilibrium titration there is undoubtedly Mg^{2+} binding beyond the X_4 stage which pulls on the preceding equilibria, and affects the overall equilibrium titrations. The effects of this additional binding can be approximated by adding the step $X_4 + Mg^{2+} \rightleftarrows X_5$ which is characterized by the apparent dissociation constant K_5.

Let the contribution to the fluorescence intensity of any given species be equal to its concentration times its relative fluorescence. This is legitimate at the low optical densities employed. We obtain

$$F_i = f_R[R]_0$$
$$F_f = f_{X_4}[R]_0 = 1.8 f_R[R]_0 \quad (13)$$
$$F = f_R[R] + f_{X_1}[X_1] + f_{X_2}[X_2] + f_{X_3}[X_3] + f_{X_4}[X_4] + f_{X_5}[X_5]$$

where F_i = initial fluorescence, F_f = final fluorescence, F = current fluorescence, and

$$[R]_0 = \text{total tRNA concentration} = [R] + [X_1] + [X_2] + [X_3] + [X_4] + [X_5] \quad (14)$$

Making use of eq 12–14 with the definition of the equilibrium constants K_i we derive

$$\theta = \frac{F - F_i}{F_f - F_i} = \frac{\left[\frac{[Mg^{2+}]}{K_1K_2} + \frac{[Mg^{2+}]^2}{K_1K_2K_3} + \frac{5[Mg^{2+}]^2}{K_1K_2K_3K_4} + \frac{5[Mg^{2+}]^3}{K_1K_2K_3K_4K_5}\right]}{5\left[1 + \frac{[Mg^{2+}]}{K_1} + \frac{[Mg^{2+}]}{K_1K_2} + \frac{[Mg^{2+}]^2}{K_1K_2K_3} + \frac{[Mg^{2+}]^2}{K_1K_2K_3K_4} + \frac{[Mg^{2+}]^3}{K_1K_2K_3K_4K_5}\right]} \quad (15)$$

Equation 15 may be used to calculate a θ *vs.* pMg curve using the values of the K_i's given in Table II and an adjustable value of K_5. This equation gives an excellent fit to the titration at 15 mM Na^+, 20° where the calculated $n = 1.79$ (observed $n = 1.75$) and calculated $pK_{app} = 5.57$ (observed $pK_{app} = 5.63$). (A value of $K_5 = 8 \times 10^{-6}$ M has been assumed.) Almost as good a fit to the data is obtained by ignoring the step(s) ascribed to K_5, the calculated curve in this instance showing some deviation from the observed points over the final 20% or so of the titration. We conclude, therefore, that the mechanism of eq 5 adequately accounts for all equilibrium and kinetic fluorescence data. Moreover the foregoing analysis makes it easy to rationalize the existence of n values in the vicinity of 1.5–3.0 for the equilibrium titrations (*cf.* Table I). This clearly arises because all of the emission changes appear to be associated with the binding of the first ions, thus giving greatest weight to these in a plot of θ *vs.* pMg.

Discussion

Binding of Mg^{2+} (or Mn^{2+}) to tRNA has also been studied by many other workers, using a wide variety of techniques. These studies have focused on the overall equilibrium binding of Mg^{2+}. Observation of the stoichiometry of binding *via* nmr

(Cohn *et al.*, 1969), esr (Danchin and Guéron, 1970), Sephadex column chromatography (Yarus and Rashbaum, 1972), heat of Mg^{2+} binding (Rialdi *et al.*, 1972), and equilibrium dialysis (Danchin, 1972; Schreier and Schimmel, 1974) has yielded a fairly consistent picture of the overall binding. It is generally found that there are a relatively small number (4–6) of divalent ions bound to specific "strong" binding sites with dissociation constants of *ca.* 10^{-5}–10^{-6} M and a larger number (15–25) of more weakly bound ions (*ca.* 10^{-3}–10^{-4} M). The 4–6 very strongly binding ions appear to bind in a cooperative fashion (Cohn *et al.*, 1969; Danchin and Guéron, 1970; Danchin, 1972; Schreier and Schimmel, 1974).

The cooperative dependence of fluorescence on $[Mg^{2+}]$, and the values of the dissociation constants obtained (*cf.* Table I), clearly indicate that the probe is responsive to Mg^{2+} binding at the interacting sites. Under the conditions of the kinetics experiments (15 mM Na^+, 20°), the value of the Hill parameter n, determined by fluorescence, is ~1.8, which suggests that two (at least) Mg^{2+} ions are responsible for the emission changes. This is confirmed by the fact that the fluorescence kinetic studies of Mg^{2+} binding are entirely consistent with a mechanism in which sequential binding of two Mg^{2+} ions accounts for the observed transient emission changes (see eq 5). The reason that binding of subsequent ions to the interacting sites is not seen is apparent from the analysis of transient fluorescence amplitudes and equilibrium parameters (see the section on Use of Kinetic Parameters to Calculate Equilibrium Titration Curves). This analysis shows that the structural change resulting from the binding of the second Mg^{2+} is sufficient to cause a saturation in the fluorescence emission, even though the nucleic acid is not saturated with respect to Mg^{2+} binding. Under ionic conditions where $n > 2$ (*cf.* Table I), the emission changes are clearly affected by Mg^{2+} binding beyond the steps depicted in eq 5. This is due to stronger relative binding of the ions subsequent to the first two and/or to saturation of fluorescence not occurring until three or four ions bind, rather than only two.

We have implicitly assumed that the cooperative ion binding detected by fluorescence represents the first ions to bind, in the cooperative sequence of four to six ions. This assumption gives the *simplest* mechanism consistent with the data. If binding of one or two ions to interacting sites (without causing emission changes) precedes steps depicted in eq 5, the rate equations for the transient emission changes become more complex and contain additional terms which are not required (or necessarily justified) by the data.[4]

The physical significance of the mechanism for cooperative binding bears some comment. It is clearly an example of a "sequential" mechanism in which binding of a ligand induces or facilitates a structural change which enables binding of a subsequent ligand. This is exactly analogous to the model of Koshland *et al.* (1966) proposed for the mechanism of cooperative binding of ligands to proteins. Our data do not fit the concerted model of Monod *et al.* (1965). For example, let us assume that the Mg^{2+}-free tRNA exists in two conformational forms, R and T, where Mg^{2+} binds with a high preference to the "R" form. If we assume that bimolecular Mg^{2+} binding steps are fast compared to the $R \rightleftarrows T$ structural change, then the single reciprocal time constant λ characteristic of the overall structural change will *decrease* with increasing Mg^{2+}. This contrasts with the observed behavior of *two* sequential structural changes, each characterized by reciprocal time constants which *increase* with the increasing Mg^{2+} (*cf.* Figures 7a and b). It also appears from the limited data on transient uv changes (*cf.* Figure 6) that these two sequential structural changes are the only significant ones that occur.

The rates of the structural changes associated with cooperative Mg^{2+} binding are very slow at 20° (see Figures 7a and b). Because of the sizable activation energies associated with these processes (see Table III), however, the rates are much faster at physiological temperatures, *i.e.*, 37°. For example, the time constant λ_2^{-1} of the slowest step in eq 5 approaches 1 sec ($[Mg^{2+}] > 5$ mM) at 37°, based on an activation energy of 33 kcal mol^{-1}. Thus, the rates observed in the present study pose no problems, as far as the ability of the tRNA to fold quickly under physiological conditions is concerned.

The question which naturally arises is the nature of the conformational changes induced by Mg^{2+} addition to the cooperative sites. It is assumed that the final conformation obtained is the native tertiary structure, which quite plausibly is similar to the crystal structure of Kim *et al.* (1973). The cloverleaf in the crystal form is folded in such a fashion that the dihydrouridine and TψC loops are in close proximity. This bringing together of chain segments might represent an unfavorable process unless some cations are able to bind strongly to stabilize the junction. This area also represents a region of unusual tRNA geometry where particularly strong cation binding sites might exist. It is easy to see that cooperative cation interactions could be associated with this locus; *e.g.*, the binding of a cation to one of the loops might stabilize and thus induce the folding over of the other loop. Experimental evidence for this suggestion is meager, but equilibrium dialysis results of Schreier and Schimmel (1974) have shown that a chain cleavage near this locus essentially eliminates cooperative binding of Mn^{2+} to yeast $tRNA^{Phe}$, whereas a cleavage in the anticodon loop does not destroy cooperativity.

The sequence of kinetic events in the Mg^{2+}-induced folding of tRNA might be envisioned as follows. A quasi-cloverleaf pairing pattern may exist in low salt solution, but without superfolding into a tertiary configuration. (Evidence for extensive order in the low salt form comes from hypochromicity measurements (D. C. Lynch, unpublished observations; *cf.* Goldstein *et al.*, 1972; Cole *et al.*, 1972).) When Mg^{2+} is added to the solution, sections of the low salt helix might have to be broken in order to form the tertiary structure. The breaking of small helical sections and subsequent structural rearrangements could reasonably have rates and activation energies commensurate with those observed (see Tables II and III).

The kinetic results reported here bear some similarity to those of Cole *et al.* (1972) who reported slow kinetic processes accompanying the addition of high amounts of Na^+ to low salt solutions of several tRNAs. Kinetic processes were monitored *via* optical density so that the changes observed were quite small. A systematic study of the Na^+ dependence of the kinetics was not made and only the slowest process was resolved. "Apparent" activation energies of 25–61 kcal mol^{-1} were found depending on the tRNA ($tRNA^{Val}$, $tRNA^{Phe}$, $tRNA^{Tyr}$, and $tRNA^{fMet}$ from *E. coli* were studied). The authors suggest that the activation energies arise from the necessity of breaking up aberrant structure in the low salt form of tRNA. This structure is envisioned as an "extended" secondary structure in which the tRNA is folded like a hairpin with the anticodon and acceptor stem helices intact, and the

[4] It is possible that rapidly equilibrating side pathways exist off of the main kinetic pathway shown in eq 5. These pathways might be of some significance in a rapid quantitative removal of metal ion from tRNA, for example.

region in the center forming whatever pairing patterns are available to it. Such an extended structure is believed to be favored in low salt because it minimizes the phosphate charge repulsion.

How does the fluorescent probe successfully monitor the structural changes accompanying Mg^{2+} binding? It is obvious that the emission changes that occur must result from a change in the environment of the probe. One possibility is that the probe is capable of intercalating into a helical section of the tRNA as well as existing as a free "unbound" label at the 3′-terminus of the chain. The tRNA conformational changes are then able to affect the equilibrium of the label between "bound" and "free" states which in turn gives emission changes. Some support for this notion is presented in the following paper (Lynch and Schimmel, 1974).

Some mention should be made of several other studies which involved probes at the 3′-end of tRNA. Such studies include the coupling of an acridine dye to the periodate oxidized 3′-adenosine (Millar and Steiner, 1966), the substitution of formycin for the 3′-adenosine (Ward *et al.*, 1969), and the attachment of a spin-label to the amino acid of *E. coli* Val-$tRNA^{Val}$ and Phe-$tRNA^{Phe}$ (Schofield *et al.*, 1970). In each case it was shown that the probe is sensitive to the tRNA structure since the signal from the label underwent thermal "melting." No systematic studies of cation binding were pursued in any of these investigations, however, and detailed comparisons with the present work cannot be made.

Fluorescence Mg^{2+} titrations have been obtained with yeast $tRNA^{Phe}$ which possesses the fluorescent Y base (Beardsley *et al.*, 1970; Robison and Zimmerman, 1971a,b). Large emission changes occur upon Mg^{2+} addition at low salt, pH 7.2 (Robison and Zimmerman, 1971a,b), but the changes appear to be centered at Mg^{2+} concentrations significantly above those necessary to titrate the strong binding sites observed here. Moreover, the transient kinetics associated with changes in Y-base fluorescence are much more rapid than observed here (R. Gamble and P. R. Schimmel, unpublished). Therefore, it seems clear that the Y base does not monitor the kinds of structural changes which are observed in the present study.

Appendix

Derivation of Rate Equations for Mechanism of Eq 5. The rate equations characterizing the two slowest steps in eq 5 are

$$-\mathrm{d}(\Delta R + \Delta X_1)/\mathrm{d}t = k_2\Delta X_1 - k_{-2}\Delta X_2 \qquad \text{(I-1)}$$

$$-\mathrm{d}\Delta X_4/\mathrm{d}t = -k_4(\Delta X_3) + k_{-4}(\Delta X_4) \qquad \text{(I-2)}$$

where (ΔX_i) is the deviation in the concentration of $[X_i]$ from its final equilibrium value $[\bar{X}_i]$. The conservation equation among tRNA species is

$$\Delta R + \Delta X_1 + \Delta X_2 + \Delta X_3 + \Delta X_4 = 0 \qquad \text{(I-3)}$$

Since the bimolecular steps are rapidly equilibrated compared to the unimolecular processes we can differentiate the equilibrium constant expressions K_1 and K_3 we obtain

$$[\bar{R}]\Delta Mg^{2+} + [\overline{Mg}^{2+}](\Delta R) = K_1\Delta X_1 \qquad \text{(I-4)}$$

or

$$\Delta R \cong [K_1/[\overline{Mg}^{2+}]]\Delta X_1$$

and

$$[\bar{X}_2]\Delta Mg^{2+} + \Delta X_2[\overline{Mg}^{2+}] = K_3\Delta X_3 \qquad \text{(I-5)}$$

or

$$\Delta X_2 \cong [K_3/[\overline{Mg}^{2+}]]\Delta X_3$$

The approximations in eq I-4 and I-5 assume that the terms involving ΔMg^{2+} are much smaller than those involving $[\overline{Mg}^{2+}]$. This follows immediately from the fact that EDTA buffering assures $(\Delta Mg^{2+}) \approx 0$ at low Mg^{2+} concentration and $(\overline{Mg}^{2+}) \gg$ (total tRNA) at all other Mg^{2+} concentrations. Substitution of eq I-4 and I-5 into eq I-3 gives

$$-\Delta X_2 = \frac{\Delta X_1(1 + K_1/[Mg^{2+}]) + \Delta X_4}{(1 + [Mg^{2+}]/K_3)} \qquad \text{(I-6)}$$

where the overbar on Mg^{2+} has been dropped. Substitution of eq I-4–I-6 into eq I-1 and I-2 gives eq 6 with the a_{ij}'s defined as eq 7a–d.

References

Amdur, I., and Hammes, G. G. (1966), Chemical Kinetics, New York, N. Y., McGraw-Hill.

Barnett, R. E., and Jencks, W. P. (1969), *J. Amer. Chem. Soc. 91*, 6758.

Beardsley, K., Tao, T., and Cantor, C. R. (1970), *Biochemistry 9*, 3524.

Bonnet, J., and Ebel, J.-P. (1972), *Eur. J. Biochem. 31*, 335.

Cohn, M., Danchin, A., and Grunberg-Manago, M. (1969), *J. Mol. Biol. 39*, 199.

Cole, P. E., Yang, S. K., and Crothers, D. M. (1972), *Biochemistry 11*, 4358.

Craig, M. E., Crothers, D. M., and Doty, P. (1971), *J. Mol. Biol. 62*, 383.

Danchin, A. (1972), *Biopolymers 11*, 1317.

Danchin, A., and Guéron, M. (1970), *Eur. J. Biochem. 16*, 532.

Eigen, M., and DeMaeyer, L. (1963), *in* Technique of Organic Chemistry, Vol. 8, Part 2, Friess, S. L., Lewis, E. S., and Weissberger, A., Ed., New York, N. Y., Interscience, p 895.

Fresco, J. R., Adams, A., Ascione, R., Henley, D., and Lindahl, T. (1966), *Cold Spring Harbor Symp. Quant. Biol. 31*, 527.

Gillam, I., Blew, D., Warrington, R. C., von Tigerstrom, M., and Tener, G. M. (1968), *Biochemistry 7*, 3459.

Goldstein, R. N., Stefanovic, S., and Kallenbach, N. R. (1972), *J. Mol. Biol. 69*, 217.

Hammes, G. G., and Haslam, J. L. (1968), *Biochemistry 7*, 1519.

Hammes, G. G., and Haslam, J. L. (1969), *Biochemistry 8*, 1591.

Hammes, G. G., and Schimmel, P. R. (1970), *Enzymes, 3rd Ed. 2*, 67.

Henley, D. H., Lindahl, T., and Fresco, J. R. (1966), *Proc. Nat. Acad. Sci. U. S. 55*, 191.

Hercules, D. M., and Rogers, L. B. (1958), *Anal. Chem. 30*, 96.

Kim, S. H., Quigley, G. J., Suddath, F. L., McPherson, A., Sneden, D., Kim, J. J., Weinzierl, J., and Rich, A. (1973), *Science 179*, 285.

Koshland, D. E., Jr., Némethy, G., and Filmer, D. (1966), *Biochemistry 5*, 365.

Laitinen, H. A. (1960), Chemical Analysis, New York, N. Y., McGraw-Hill.

Lindahl, T., Adams, A., and Fresco, J. R. (1966), *Proc. Nat. Acad. Sci. U. S. 55*, 941.

Lynch, D. C. (1973), Ph.D. Thesis, M.I.T.

Lynch, D. C., and Schimmel, P. R. (1974), *Biochemistry 13*, 1852.

Millar, D. B., and Steiner, R. F. (1966), *Biochemistry 5*, 2289.

Monod, J., Wyman, J., and Changeux, J. P. (1965), *J. Mol. Biol. 12*, 88.
Pearlmutter, A. F., and Stuehr, J. (1968), *J. Amer. Chem. Soc. 90*, 858.
Pörschke, D., and Eigen, M. (1971), *J. Mol. Biol. 62*, 361.
Reeves, R. H., Cantor, C. R., and Chambers, R. W. (1970), *Biochemistry 9*, 3993.
Rialdi, G., Levy, J., and Biltonen, R. (1972), *Biochemistry 11*, 2472.
Robison, B., and Zimmerman, T. P. (1971a), *J. Biol. Chem. 246*, 110.
Robison, B., and Zimmerman, T. P. (1971b), *J. Biol. Chem. 246*, 4664.
Rossi-Fanelli, A., Antonini, E., and Caputo, A. (1964), *Advan. Protein Chem. 19*, 74.
Rossotti, F. J. C., and Rossotti, H. (1961), The Determination of Stability Constants, New York, N. Y., McGraw-Hill.
Saneyoshi, M., Harada, F., and Nishimura, S. (1969), *Biochim. Biophys. Acta 190*, 264.
Schofield, P., Hoffman, B. M., and Rich, A. (1970), *Biochemistry 9*, 2525.
Schreier, A. A. (1973), Ph.D. Thesis, M.I.T.
Schreier, A. A., and Schimmel, P. R. (1972), *Biochemistry 11*, 1582.
Schreier, A. A., and Schimmel, P. R. (1974), *J. Mol. Biol.* (in press).
Takahashi, K. (1961), *J. Biochem. (Tokyo) 49*, 1.
Tao, T., Nelson, J. H., and Cantor, C. R. (1970), *Biochemistry 9*, 3514.
Ward, D. C., Reich, E., and Stryer, L. (1969), *J. Biol. Chem. 244*, 1228.
Willick, G. E., and Kay, C. M. (1971), *Biochemistry 10*, 2216.
Yang, S. K., Söll, D. G., and Crothers, D. M. (1972), *Biochemistry 11*, 2311.
Yarus, M., and Barrell, B. G. (1971), *Biochem. Biophys. Res. Commun. 43*, 729.
Yarus, M., and Berg, P. (1969), *J. Mol. Biol. 42*, 171.
Yarus, M., and Rashbaum, S. (1972), *Biochemistry 11*, 2043.

Effects of Abnormal Base Ionizations on Mg^{2+} Binding to Transfer Ribonucleic Acid as Studied by a Fluorescent Probe†

Dennis C. Lynch‡ and Paul R. Schimmel*

ABSTRACT: The naphthoxyl probe attached to the 3′-end of isoleucyl-$tRNA^{Ile}$ (see Lynch, D. C., and Schimmel, P. R. (1974), *Biochemistry 13*, 1841) has been used to study the pH dependence of Mg^{2+} binding at "cooperative" sites. The apparent Mg^{2+} affinity is strongly pH dependent; *e.g.*, it is *ca.* tenfold and 100-fold weaker at pH 6 and pH 4.7, respectively, than at pH 7.5. This effect is due to abnormally high base p*K*'s in the "aberrant" structure(s) formed in low salt, Mg^{2+}-free solutions. The emission of the probe is sensitive to the ionization of one of these sites, probably a cytidylic acid moiety near the 3′-end. Addition of sufficient Mg^{2+} sharply lowers the abnormal p*K*'s to more typical values. The kinetics of Mg^{2+} addition at pH 6 appears to follow essentially the same mechanism as at pH 7.5—two slow unimolecular changes coupled to rapid Mg^{2+} binding steps. However, the Mg^{2+}-induced structural changes are slower, have somewhat higher activation energies, and are thermodynamically less favored at pH 6. These effects apparently arise from the greater stability of aberrant form(s) brought about by base protonations, and they largely account for the weaker apparent binding of Mg^{2+} observed by fluorescence at pH 6 as opposed to pH 7.5. Ultraviolet absorption data corroborate many of the findings. Preliminary results with $tRNA^{Ala}$ (*Escherichia coli*) labeled with the probe are similar to those obtained with $tRNA^{Ile}$, thus suggesting that the results obtained may be rather general.

In the preceding paper (Lynch and Schimmel, 1974), it was shown that the fluorescence emission of a naphthoxyl group attached to the 3′-end of $tRNA^{Ile}$ is sensitive to the binding of Mg^{2+} to "interacting" or "cooperative" sites on the nucleic acid. Two slow unimolecular structural changes occur as Mg^{2+} is bound to these sites; these changes have large activation energies and are probably due to the breakdown of aberrant structures formed in the absence of Mg^{2+} (see Cole *et al.*, 1972). Since the structural changes induced by Mg^{2+} binding are thermodynamically favorable, they serve to increase the apparent strength of binding of Mg^{2+}. This accounts for the high affinity of Mg^{2+} binding to these sites.

At pH 6 we were surprised to learn that the binding of Mg^{2+} observed by fluorescence is significantly weaker than that observed at pH 7.5 (Lynch and Schimmel, 1974), even though there are no obvious base or phosphodiester ionizations in this pH range. The results presented below demonstrate that abnormal p*K*'s (on bases) are present on tRNA and that protonation of these sites leads to an increased stabilization of the "aberrant" structure(s) formed in low salt. Addition of Mg^{2+} sharply lowers the abnormal p*K*'s and encourages proper folding of the tRNA, although the folding process itself is somewhat slower and goes with higher activation energies at the more acid pH (pH 6) than at pH 7.5. The decreased thermodynamic preference for the Mg^{2+}-induced

† From the Departments of Biology and Chemistry, Massachusetts Institute of Technology, Cambridge, Massachusetts 02139. *Received October 23, 1973.* This work was supported by grant no. GM-15539 from the National Institutes of Health. Material for this manuscript was taken from the Ph.D. thesis of Dennis C. Lynch (Massachusetts Institute of Technology, 1973).

‡ Present address: Division of Biology, California Institute of Technology, Pasadena, Calif. 91109. Predoctoral Fellow of the National Institutes of Health, 1970–1973.